Turk J Pharm Sci 2025;22(2):91-103
DOI: 10.4274/tjps.galenos.2025.66350

ORIGINAL ARTICLE

Formulation and Optimization of Pyrazinamide-Loaded Solid Lipid Nanoparticles by Employing a Design of Experiments Approach

Nimitt CHOKSHI, Preksha VINCHHI, Shreyansh CHAUHAN, Mayur PATEL*

Nirma University Institute of Pharmacy, Department of Pharmaceutics, Gujarat, India

ABSTRACT

Objectives: Tuberculosis (TB) remains a major worldwide health challenge causing morbidity and mortality, necessitating novel approaches for its effective therapy. Pyrazinamide (PYZ), a nicotinamide analogue, is a key frontline drug significantly involved in the treatment of TB. However, its dose-dependent hepatotoxicity is a major concern that needs to be addressed. The aim of the current research was to develop PYZ-loaded solid lipid nanoparticles (PYZ-SLNs) as a potential therapeutic intervention for treating TB.

Materials and Methods: The PYZ-SLNs were formulated by a high-pressure homogenization technique and optimized using a 23-factorial design. The drug concentration, emulsifier concentration, and homogenization cycles were considered critical formulation and processing parameters to study their effects on essential attributes of quality of PYZ-SLNs, i.e., entrapment efficiency (EE%), drug loading (DL%), and particle size.

Results: The optimized PYZ-SLNs showed a particle size of 401±08 nm, EE% of 86.24±1.15, DL% of 14.38±0.85. The *in vitro* lipolysis studies revealed that PYZ-SLNs exhibited an anti-lipolytic effect due to stabilization by poloxamer 188. Moreover, the *in vitro* gastrointestinal (GI) stability results demonstrated that the PYZ-SLNs were stable in GI tract media (at pH 1.2, pH 4.5, pH 6.8, and pH 7.4). The *in vitro* drug release studies showed the best fit with the Hixon-Crowell model. The accelerated stability studies revealed no significant changes in PYZ-SLNs for 6 months.

Conclusion: PYZ-SLNs could be a promising carrier for the treatment of TB via the oral intestinal lymphatic pathway, circumventing its hepatic first-pass metabolism and thereby preventing hepatic adverse effects.

Keywords: Full factorial design, lipolysis model, long-chain lipids, lymphatic delivery, drug release kinetics

INTRODUCTION

Tuberculosis (TB) is a major worldwide health issue causing morbidity and mortality. It is an ailment that strikes in conditions of malnutrition, poverty, and limited healthcare access. Approximately 10.6 million people developed TB, and 1.3 million people died from TB in 2022, as per the World Health Organization Global TB Report. Primarily, developing countries such as India, Bangladesh, Pakistan, Philippines, Nigeria, and Indonesia bear the brunt of the worldwide TB burden.[1] The currently available TB treatment lasts from 6 months to 12 months, depending on its type.[2-6] The drug treatment for TB is complex due to its adverse effects, multiple drug regimens, and longer duration. Thus, effective drug formulations are necessary that can provide sustained release over a ,more extended period and thereby increase medication adherence in patients.[7]

A nicotinamide analogue, pyrazinamide (PYZ), is an essential frontline drug utilized for TB treatment. PYZ has a noteworthy role in shortening the TB treatment schedule from a duration of 9 to 12 months to a schedule of 6 months.[8] The capability of PYZ to shorten the schedule is due to its activity against a population of persistent tubercle bacilli dwelling in acidic pH

***Correspondence:** drmayurmpatel@gmail.com, **ORCID-ID:** orcid.org/0000-0002-9057-5769
Received: 06.03.2024, **Accepted:** 07.02.2025 **Publication Date:** 14.05.2025

Cite this article as: CHOKSHI N, VINCHHI P, CHAUHAN S, PATEL M. Formulation and optimization of pyrazinamide-loaded solid lipid nanoparticles by employing a design of experiments approach. Turk J Pharm Sci. 2025;22(2):91-103

environments that are not destroyed by other TB drugs. The acidic pH facilitates the intracellular accumulation of pyrazinoic acid, the active derivative of PYZ formed by the conversion of PYZ by pyrazinamidase. Due to high dosing frequency and high drug payload, the regimen for PYZ bactericidal activity is limited to two months. A PYZ dose of 15-30 mg/kg, or 1.5 to 2 g (depending on the patient's weight) is generally given. However, dose-dependent hepatotoxicity is a severe adverse effect of PYZ. Furthermore, major adverse effects of PYZ also include gouty arthritis, hyperuricemia, and, in rare cases, nephritis.[2,3,6,9,10]

Several research studies have been conducted on formulating and developing nano-carriers to deliver PYZ, namely, liposomes,[9] colloidosomes,[11] polymeric nanoparticles,[6,12] *etc*. Liposomes are potential carriers offering unique advantages; however, issues such as rapid leakage of water-soluble drugs, low encapsulation efficiency, instability in plasma, and poor storage stability persist.[12] Moreover, polymeric nanocarriers often require organic solvents in their fabrication, leading to toxicity and environmental risk.[13] Additionally, researchers explore inhalation therapy to deliver PYZ. However, challenges in using specialized delivery devices and implementing them on a large scale are some of the drawbacks that need to be addressed.[14]

The oral route is the most convenient for drug delivery. The key contributing factors affecting the oral bioavailability of drugs are gastric mean residence time, pH of the gastrointestinal (GI) tract, and drug solubility and permeability. Moreover, the pre-systemic metabolism also affects the bioavailability of drugs. The lymphatic pathway is a preferable alternative for avoiding first-pass metabolism. Several colloidal nano-carriers such as nano-micelles, self-emulsifying delivery systems, polymeric nanoparticles, liposomes, microemulsions, and solid lipid nanoparticles (SLNs) have been explored for achieving oral delivery via intestinal lymphatic transport.[15-17]

SLNs have emerged as promising nanoparticles as they amalgamate the benefits of all colloidal carriers mentioned and thereby improve the effectiveness of encapsulated drugs. They enhance the drug's lymphatic uptake. They are taken up *via* lymphatic circulation and enter blood vessels *via* jugular and subclavian veins, thus preventing the first-pass metabolism of the drug, and thereby reducing hepatic adverse effects.

Incorporating PYZ in SLNs would also promote drug efficacy, lessen the drug dose, and provide a sustained release.[18-20] Furthermore, it has been reported that the drug must have log $P \geq 4.7$ to be suitable for lymphatic uptake. PYZ exhibits a log *P* of -1.884; hence, it cannot enter the lymphatics and thereby undergoes hepatic first-pass metabolism.[21] Thus, based on the facts above, there is a dire need to develop therapeutic strategies that reduce PYZ hepatic toxicity.

To surmount the limitations associated with PYZ therapy, we propose an encapsulation of PYZ in SLNs to reduce hepatic adverse effects. The fabricated PYZ-SLNs contain long-chain lipids that facilitate absorption through the lymphatic system compared to medium or short-chain lipids. Moreover, the SLNs were developed utilizing poloxamer 188 (surfactant), which develops a steric crown on the SLNs surface, thus decreasing their contact with pancreatic and gastric lipase. Thus, poloxamer 188 plays a significant role in maintaining the integrity of PYZ-SLNs during its migration *via* the GI tract into the lymphatic system (Figure 1).[22]

MATERIALS AND METHODS

Materials

PYZ (99% pure) was obtained as a gift sample from S. Kant Healthcare Ltd., Mumbai, India. Stearylamine and stearic acid were acquired from Himedia Laboratories in Mumbai, India. Compritol 888 ATO (Glyceryl di- and tri-behenate) was acquired as a kind gift from Gattefosse India Pvt. Ltd., Mumbai, India. Glyceryl monostearate was donated by Hallstar, USA. Softisan 154 and Dynasan (114, 116, and 118) were donated by CremerOleo, Germany. Crodamol cetyl palmitate was acquired as a gratis sample from Croda, Mumbai, India. Tween 80, tween 20, sorbitan monooleate (span 80), and sorbitan monolaurate (span 20) were acquired from Central Drug House (CDH) Pvt. Ltd., New Delhi, India. Cremophor EL, cremophor RH 40, poloxamer 407 (P407), poloxamer 188 (P188), and solutol HS 15 samples were acquired as samples from BASF India Ltd., Mumbai, India. Soy Lecithin (Source: Soy), lipoid S 75 phospholipon 90 H, and phospholipon 90 G were acquired as samples from Lipoid GmbH, Germany. Sephadex G-50 (grade: coarse) was procured from MP Biomedicals, USA. Mannitol was acquired from CDH, New Delhi, India. The solvents used were of high performance liquid chromatography (HPLC) grade, and all additional chemicals were of analytical grade.

Surfactants and solid lipids screening

The lipids were heated to 10 °C higher than their melting temperature in a glass vial. PYZ (in increments of 2 mg) was incorporated into the melted lipid, which was stirred at

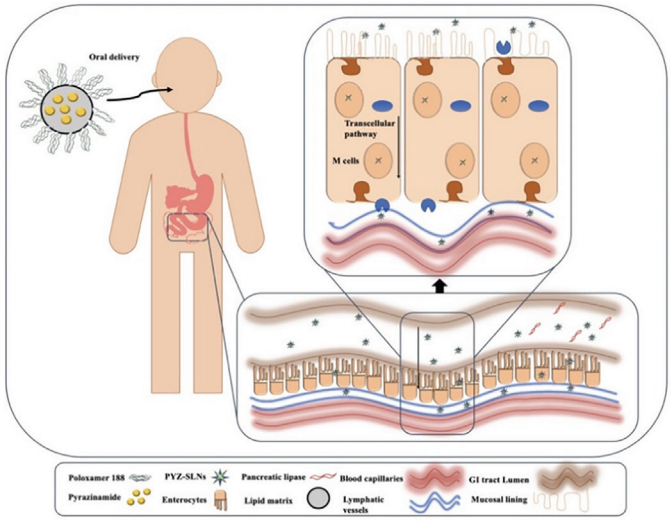

Figure 1. Schematic representation of the mechanism of oral absorption of PYZ-SLNs *via* the intestinal lymphatic system

PYZ-SLNs: Pyrazinamide-loaded solid lipid nanoparticles

100 rpm for 24 h by employing a water bath incubator shaker (EIE Instruments Pvt. Ltd., Ahmedabad). To confirm whether insoluble drug crystals were present or absent, the lipid melts were examined against a black-and-white background. The solubility of the drug was also assessed in several surfactant solutions (1% *w/v*) that were kept at a temperature of 25±2 °C. All the above-mentioned studies were carried out in triplicate sets.[23-26]

Preparation of PYZ-SLNs

The high-pressure homogenization method was used for the fabrication of PYZ-SLNs.[27-29] In brief, soy lecithin (0.3% *w/v*), stearyl amine (0.1% *w/v*), and stearic acid (1% *w/v*) were heated (10 °C above the melting point of the lipids) in a beaker using a water bath to obtain a uniform lipid phase. In the lipid melt phase, PYZ (30% *w/w*) was added and dissolved with constant stirring. Poloxamer 188 (3% *w/v*) was melted at a temperature similar to the lipid phase to obtain an aqueous surfactant solution. A high-speed stirrer (12000 rpm) (RQ 122/D Remi mechanical stirrer, Remi Mumbai, India) was used to mix aqueous surfactant solution and melted lipid phase, to form a pre-emulsion. A high-pressure homogenizer (GEA Lab Homogenizer PandaPLUS 200, Niro Soavi, Italy) was employed for the nanonization of pre-emulsion. It was subjected to 12 homogenization cycles at 1200 bar pressure in the homogenizer. The formulated SLNs were then lyophilized after the addition of cryoprotectant (Mannitol: 5% *w/v*) employing a bench-top freeze-dryer (FD-10-MR, Labfreez Instruments, Beijing, China) and were stored in a cool place.[26,30-35]

Statistical analysis

Statistical optimization of PYZ-SLNs

The PYZ-SLNs were optimized for various processing and formulation variables by applying the design of experiments using Design Expert software (Stat-Ease, Inc., Minneapolis, MN, USA). The preliminary batches (data not shown) were fabricated and characterized to investigate the formulation and processing variables influencing the PYZ-SLNs. A 2^3 full factorial design (two levels and three factors) was applied to optimize PYZ-SLNs. A 2^3 full factorial design estimates the impact of three factors (screened *via* preliminary trials) at two levels (high and low) on the dependent variables.

PYZ-SLNs characterization studies

Determination of particle size, polydispersity index (PDI), and zeta potential (ZP)

The particle size analysis was conducted by employing Zetasizer Nano ZS90 (Malvern Panalytical Ltd., Malvern, UK), which functions based on the principle of dynamic light scattering. The sample was diluted, for particle size analysis, to the required concentration using water for injection. Particle size distribution results were acquired, indicating the PDI of formulated PYZ-loaded SLNs. Each sample had a run time of 120 seconds. The ZP calculates the particle's electrophoretic mobility in an electric field using about 12 to 15 runs for every measurement. All the above-mentioned studies (D90, PDI, and ZP) were carried out in triplicate sets.[24,25,33-35]

Evaluation of DL% and EE%

The DL% and EE% of the PYZ-SLNs were estimated based on the size exclusion chromatography principle by utilizing the Sephadex G-50 minicolumn and centrifugation technique (as discussed elsewhere).[34,36]

The drug-loaded SLNs, after centrifugation, collected from Sephadex G-50 mini column were diluted (20 times) using a 2:1 ratio of dichloromethane, methanol to determine the entrapped drug ($W_{entrapped}$). A validated HPLC method was utilized to analyze the EE% of the aforementioned sample. All the above-mentioned procedures were carried out in triplicate. The following formula was used to calculate the EE%:

$$EE\% = \frac{W_{entrapped}}{W_{total}} \times 100 \quad \text{(Equation 1)}$$

Where $W_{entrapped}$ is the amount of entrapped PYZ in the SLNs (Separated *via* Sephadex G-50 column), W_{total} is the whole PYZ quantity that was added into the formulation.

The following formula was used to calculate the DL%:[37]

$$DL\% = \frac{W_{entrapped}}{\text{Quantity of solids added}} \times 100 \quad \text{(Equation 2)}$$

Differential scanning calorimetry (DSC) analysis

A Shimadzu DSC 60 A (Kyoto, Japan) linked to a TDA trend line program was utilized for calorimetric analysis. Samples were weighed (5 mg) in an aluminum pan, while an empty aluminum pan served as the reference. Thermograms were scanned at 10 °C per minute from 40 °C to 300 °C. Thereafter, the samples were cooled down to 40 °C using liquid nitrogen.[26,32-34,38]

Transmission electron microscopy (TEM) analysis

The PYZ-SLN's morphology was examined by using a CM-200 TEM (Philips, the Netherlands). On Formvar-coated TEM grids (Ted Pella, Redding, CA), SLNs (diluted 50X) were mounted and then negatively stained with phosphotungstic acid. The PYZ-SLNs sample was dried for 5 min at 25 °C and then observed using a TEM with a resolution of 0.23 nm at 200 kV.[19,24-26,33,34,39,40]

Powder X-ray diffraction (PXRD) studies

To investigate the crystallinity of PYZ and the SLNs' structure after preparation, an X-ray diffractometer (Bruker D8 Discover, Germany) was used. The diffraction patterns of pure PYZ, stearic acid (solid lipid), blank SLNs, and optimized PYZ-SLNs (batch 11) were analyzed. The samples (500 mg) were kept in the sample compartment and exposed to Ni-filtered Cu Kα-radiation at a wavelength of 1.5406 Å at 30 kV, 10 mA. Each diffractogram was recorded from 10° to 40° two theta angles, and plots (intensity *vs.* 2θ) were generated utilizing software OriginPro 2017 (OriginLab Corporation, USA).[24,25,33,34,40]

In vitro characterization studies of PYZ-SLNs

In vitro release study

Using the dialysis membrane method, the *in vitro* release from PYZ-SLNs was conducted in various solutions: 0.1 N HCl (pH

1.2) to mimic gastric pH phosphate-citrate buffer (pH 4.5) to mimic endosomal alveolar macrophage and phosphate buffer (pH 6.8 and 7.4) to mimic intestinal pH.[41-45] The volume of various release media for conducting the *in vitro* release study was 100 mL. The freeze-dried SLNs (comprising the 10 mg equivalent of entrapped PYZ) were added to the dialysis tube (molecular weight cut-off 12-14 KDa, HiMedia Laboratories Pvt. Limited, Mumbai) for the investigation. The beaker containing dialysis tubing suspended in the media was maintained at 37.0±0.5 ˚C with magnetic stirring (5-MLH Remi, Remi labworld, India) at a speed of 100 rpm. The 5 mL aliquots were drawn at predetermined time points (0, 1, 2, 4, 6, 8, 12, 24, 36, 48, 60, 72, 96, and 120 hours) and replenished with an equal amount of fresh release media to sustain the sink conditions. A validated HPLC technique was used to analyze the samples and determine the quantity of drug released.[25,26,33,34]

Drug release kinetics

The drug release data were further subjected to drug dissolution (DD) solver to determine the drug release kinetics.[46] Various mathematical models, namely first order, zero order, Higuchi, Weibull, the Hixon-Crowell, and the Korsemeyer-Peppas were evaluated to determine the drug release mechanism from SLNs. The release data were fitted to all the above-mentioned models in the DD solver program and the scatter plots were generated with the fitted curve. The model with the highest R-square value and highest *f*-value was the best fit for dissolution profiling. The formula for the models to which the release data were fitted is mentioned below:

$$\text{First order: } F = 100 \cdot (1 - e^{-k1 \cdot t}) \quad \text{(Equation 3)}$$

$$\text{Zero order: } F = k_0 \cdot t \quad \text{(Equation 4)}$$

$$\text{Higuchi: } F = k_{\text{H}} \cdot t^{0.5} \quad \text{(Equation 5)}$$

$$\text{Weibull: } F = F_{\max} \cdot \left[1 - e^{-\frac{(t-Ti)^{\beta}}{\alpha}}\right] \quad \text{(Equation 6)}$$

$$\text{Hixon-Crowell: } F = 100 \cdot [1 - (1 - k_{\text{HC}} \cdot t)^3] \quad \text{(Equation 7)}$$

$$\text{Korsemeyer-Peppas: } F = k_{\text{KP}} \cdot t^n \quad \text{(Equation 8)}$$

Where, in all models, F is the fraction (%) of drug released in time t, k_1 is first order release constant, k_0 is zero order release constant, is the Higuchi release constant, is the maximum drug released at infinite time, α (scale parameter) defines the time scale of the process, β (shape parameter) characterizes a curve as exponential, sigmoid, or parabolic; k_{HC} is release constant in the Hixson-Crowell model, is the korsemeyer-peppas release constant incorporating the geometric and structural characteristics of the formulation, and *n* is the diffusional exponent defining the release mechanism.[47]

In vitro lipolysis test

The *in vitro* lipolysis test of PYZ-SLNs was conducted as per the previously described procedure using simulated empty-state intestinal conditions.[48] A lipolytic medium was prepared and reacted with the formulated PYZ-SLNs. It contained calcium chloride (5 mM), sodium taurodeoxycholate (5 mM), sodium chloride (150 mM), soy lecithin (1.25 mM), pancreatic lipase (0.525 g/300 IU/mL), and sodium dodecyl sulphate (0.5% *w/v*). The lipolytic medium was buffered with tris-maleate (pH 6.8). Herein, simulated digestive media (14 mL) was mixed with PYZ-SLNs (6 mL). The above blend was stored at 37±0.5 ˚C in a thermostatic water bath. The entire lipolysis process was maintained at pH 6.8 by using an Auto Titrator (Titra+, LabIndia Analytical Instruments Pvt. Ltd., Thane, India). The autotitrator used 200 mM sodium hydroxide to counterbalance the fatty acid generated by the lipid digestion. When the pH change at 15 minute intervals was less than 0.05 units, the digestive process was considered to be complete.

$$\textit{Extent of lipolysis } (\%) = \frac{V \times C \times M.W}{3 \times \rho \times v} \times 100 \quad \text{(Equation 9)}$$

Where V is the titrant volume utilized amidst the digestion at 6.8 pH, C is the titrant concentration, M.W denotes the lipids molecular weight (g/mol) utilized for the formulation of SLNs, 3 describes that one triglyceride molecule can release a maximum of 3 fatty acids, ρ indicates the lipid density (g/mL), ν is the lipids volume in SLNs within the lipolysis medium.[24-26,33,34]

In vitro investigation of GI stability of PYZ-SLNs

GI stability of PYZ-SLNs was assessed by determining their EE%, PDI, and particle size across different pH ranges, viz. pH 1.2 (0.1 N HCl), pH 4.5 (sodium acetate buffer), pH 6.8 (PBS), and pH 7.4 (PBS), simulating the GI physiology of humans. To assess the stability of the formulated PYZ-SLNs, they were kept at pH 1.2 and 4.5 for 2 h, and incubated at pH 6.8 and 7.4 for 6 h.[19,49,50]

Stability analysis of PYZ-SLNs

The stability studies of the optimized lyophilized PYZ-SLNs were conducted according to the previously reported literature.[19,51] The lyophilized PYZ-SLNs were stored in amber-colored glass vials, sealed, and placed in an upright position in a stability chamber (Nova Instruments Pvt. Ltd. in Ahmedabad). Thereafter, the SLNs were stored at 8 ˚C, 30±2 ˚C/65±5% RH (intermediate conditions), and 40±2 ˚C/75±5% RH (accelerated conditions) for 6 months to assess their stability. At predetermined intervals, namely, initial, 1 month, 3 months, and 6 months, samples were investigated for ease of redispersibility, any alterations in physical appearance, EE%, PDI, and particle size.[24-26,32,33]

RESULTS

Lipid excipients and surfactants screening

Solid lipids screening

The solid lipid was selected based on the criterion that the drug has maximum solubility in that lipid. PYZ has a log *p* of -1.884 as it is lipophilic in nature. The results showed that stearic acid had the highest solubility of PYZ (Figure 2A). The partitioning of PYZ in various solids was evaluated.[23] Stearic acid was selected for developing PYZ-SLNs because PYZ partitioning was highest in stearic acid.

Screening of surfactants

The surfactant was selected based on the least solubility of PYZ in it. As shown in Figure 2B, the investigation was carried out using different surfactant solutions (1% *w/v*). Drug moieties are incorporated in the lipid matrix and are strongly associated with the solid lipid core due to surfactants with low drug solubility. It was necessary to select surfactants with the lowest solubility of PYZ. Drug moieties are materialized in the lipid matrix and are strongly associated with the solid lipid core by surfactants having a low drug solubility.[33,34] It was necessary to select surfactants having the least solubility for PYZ. The PYZ solubility was found to be highest in polysorbate 80 (20 mg/mL), followed by cremophor RH40 (18 mg/mL), polysorbate 40 (16 mg/mL), polysorbate 20 (16 mg/mL), and cremophor EL (16 mg/mL). PYZ was found to be moderately soluble in poloxamer 407 (14 mg/mL) and solutol HS15 (14 mg/mL). The solubility of PYZ in P188 was the lowest (12 mg/mL). Thus, P188 was selected for formulating PYZ-SLNs.

It has been reported that P188 provides an anti-lipolytic effect in the GI tract. A steric crown is created on SLNs surface, which reduces the interaction of SLNs with pancreatic and gastric lipase.[50-52] Batches CSP2 (1% *w/v* P188) and CSP3 (3% *w/v* P188) were subjected to an *in vitro* lipolysis study. Batch CSP2 degraded by 21.23±1.86%, while batch CSP3 degraded by 10.12±0.69% (Figure 2C). Thus, 3% *w/v* P188 was selected for the optimization of PYZ-SLNs as it resulted in minimum lipolysis.

PYZ-SLNs optimization by response surface methods

Optimization of PYZ-SLNs utilizing 2^3 factorial design

Based on the preliminary trial results (data not shown), it was observed that among various formulation and process variables, the parameters viz. homogenization cycles, emulsifier concentration, and drug concentration demonstrated significant impact on particle size, DL%, and EE% of PYZ-SLNs. The emulsifier concentration influenced particle size and EE%, while the drug concentration primarily impacted DL% and EE%. The homogenization cycles impacted the EE% and particle size of PYZ-SLNs. To comprehensively optimize the PYZ-SLNs, these primary observations were taken into account, and a 2^3 factorial design (two levels and three factors) was applied, as shown in Table 1 and Table 2. The following mathematical model was used to derive equations showing the link between independent and dependent variables:

$$Y = B_0 + B_1X_1 + B_2X_2 + B_3X_3 + B_{12}X_1X_2 + B_{13}X_1X_3 + B_{23}X_2X_3 + B_{123}X_1X_2X_3 \quad \text{(Equation 10)}$$

Where X_1, X_2, and X_3 are the factors (chosen from primary studies), Y_i is the dependent variable, B_1 to B_{33} is the regression coefficients range and B_0 is the intercept.

3D response surface plots were generated, and data were investigated by employing Design-Expert 10 software (version 10.0.6) (Stat-Ease, Inc., Minneapolis, MN, USA). To identify a design space with higher desirability, restraints were applied to responses.

The responses [particle size (D90), EE%, and DL%] achieved at various levels of the independent variables (X_1, X_2, and X_3) were put through multiple linear regression to obtain second-order polynomial Equations (11), (12), and (13). The equations are mentioned below:

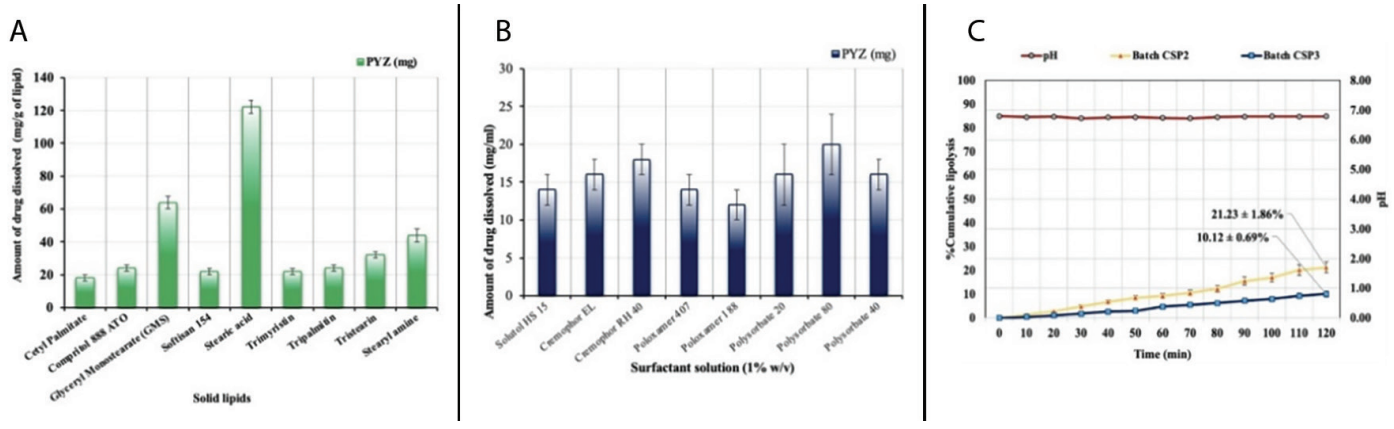

Figure 2. Solubility studies of PYZ in (A) solid lipids, (B) surfactant solutions (1% *w/v*), and (C) % cumulative lipolysis of formulation batches *versus* time profile (mean ± SD, n=3)

PYZ: Pyrazinamide, SD: Standard deviation

$$Y_1 = +446.30 + 0.28 * X_1 - 10.42 * X_2 - 26.09 * X_3 + 3.79 * X_1 * X_2 + 4.51 * X_1 * X_3 - 7.57 * X_2 * X_3 - 6.24 * X_1 * X_2 * X_3 \quad \text{(Equation 11)}$$

$$Y_2 = +83.55 + 1.03 * X_1 + 1.38 * X_2 - 0.51 * X_3 + 0.38 * X_1 * X_2 + 0.15 * X_1 * X_3 - 0.31 * X_2 * X_3 + 0.076 * X_1 * X_2 * X_3 \quad \text{(Equation 12)}$$

$$Y_3 = +12.08 + 2.28 * X_1 + 0.32 * X_2 - 0.19 * X_3 + 0.072 * X_1 * X_2 + 0.011 * X_1 * X_3 - 0.21 * X_2 * X_3 - 0.043 * X_1 * X_2 * X_3 \quad \text{(Equation 13)}$$

The equations signify the influence of X_1, X_2, and X_3 (independent variables) on Y_1, Y_2, and Y_3 (dependent responses). The correlation coefficient R^2 values were established to be 0.9484, 0.7094, and 0.9317 for dependent responses Y_1, Y_2, and Y_3, respectively, signifying a good match.

Table 1. 2^3 factorial design-independent and dependent variables

	Factors	Coded levels	
	Independent variables	Low level (-1)	High level (+1)
X_1	Drug concentration (*w/w* %)	10	30
X_2	Emulsifier concentration (*w/v* %)	0.2	0.3
X_3	Homogenization cycles	8	12
	Dependent variables	Constraints	
Y_1	D90 (nm)	D90<500 nm	
Y_2	Entrapment efficiency %	Maximum	
Y_3	Drug loading %	Maximum	

The impact of factors and independent variables on particle size is shown in Figure 3A-C. Equation (11) indicates that the X_2 and X_3 variables have a notable inverse effect on the PYZ-SLNs particle size. This suggests that the particle size (D90) of PYZ-SLNs is reduced with increasing homogenization cycles (X_3). The possible cause of the decrease in particle size might be the cavitation forces in the high-pressure homogenizer leading to the reduction of PYZ-SLNs to nano-scale size.[53,54] Moreover, the particle size of PYZ-SLNs reduces with an increase in emulsifier (X_2) concentration. This might be owing to increased stabilization of pre-emulsion by an emulsifier, leading to a diminution in particle size as well as its aggregation.[53]

The impact of the factors on EE% is represented in Figure 3D-F. It is evident from Equation (12) that factors X_1 and X_2 have a positive impact, whereas factor X_3 has a negative impact on EE% of PYZ-SLNs. The direct correlation between the drug concentration and EE% is described by the Equation. The EE% increases with an increase in drug concentration, which might be due to the increased drug availability for accommodation in a lipid matrix. The EE% rises as the emulsifier (X_2) concentration increases. The high drug solubilization and incorporation into the lipid core could be responsible for an increase in EE%.[53,55] The EE% was negatively impacted by homogenization cycles (X_3). The EE% decreased as the number of homogenization cycles increased. This might be owing to the increased surface area of particles caused by the cavitational forces generated with increased cycles of homogenization, resulting in drug leaching during SLN formation.[53,54] The impact of factors on response DL% is represented in Figure 3G-I. It is clear from Equation (13) that the variables X_1 and X_2 have a positive impact on DL%. The increase in drug concentration was attributed to more drug able to be incorporated into the lipid matrix. Furthermore, the drug is more solubilized in the lipid matrix with the addition of an emulsifier. Thus, an increase in emulsifier concentration increases the DL%. It was found that as the homogenization cycles increased, the DL% was reduced. This could be the

Table 2. Components of experimental batches (mean ± SD, n=3)

Batch no.	(X_1)	(X_2)	(X_3)	Particle size (nm) (Y_1)		EE (Y_2) %		Drug loading (Y_3) %	
				Observed	Predicted	Observed	Predicted	Observed	Predicted
P1	-1	-1	-1	521±15	517.99	81.2±3.1	80.62	5.71±0.61	5.27
P2	1	-1	-1	470±9	460.98	84.7±2.7	82.96	15.21±1.15	13.89
P3	-1	1	-1	453±10	452.12	82.4±1.4	82.18	5.81±0.37	5.64
P4	1	1	-1	478±14	475.35	87.6±2.4	86.93	15.70±1.24	15.18
P5	-1	-1	1	417±12	416.48	80.1±0.4	79.79	5.24±0.26	4.99
P6	1	-1	1	447±11	445.43	83.6±2.7	82.68	14.80±1.52	14.04
P7	-1	1	1	395±8	395.19	79.4±3.4	79.21	5.21±0.62	5.05
P8	1	1	1	404±6	404.56	86.3±1.7	85.74	14.82±0.96	14.33
P9*	0	-0.5	-0.5	439±14	433.25	81.9±2.5	83.29	10.70±0.58	11.98
P10*	0	0	0.5	440±12	462.66	79.2±4.2	83.04	9.12±0.59	11.96

*: Checkpoint batches, SD: Standard deviation, no.: Number, EE: Entrapment efficiency

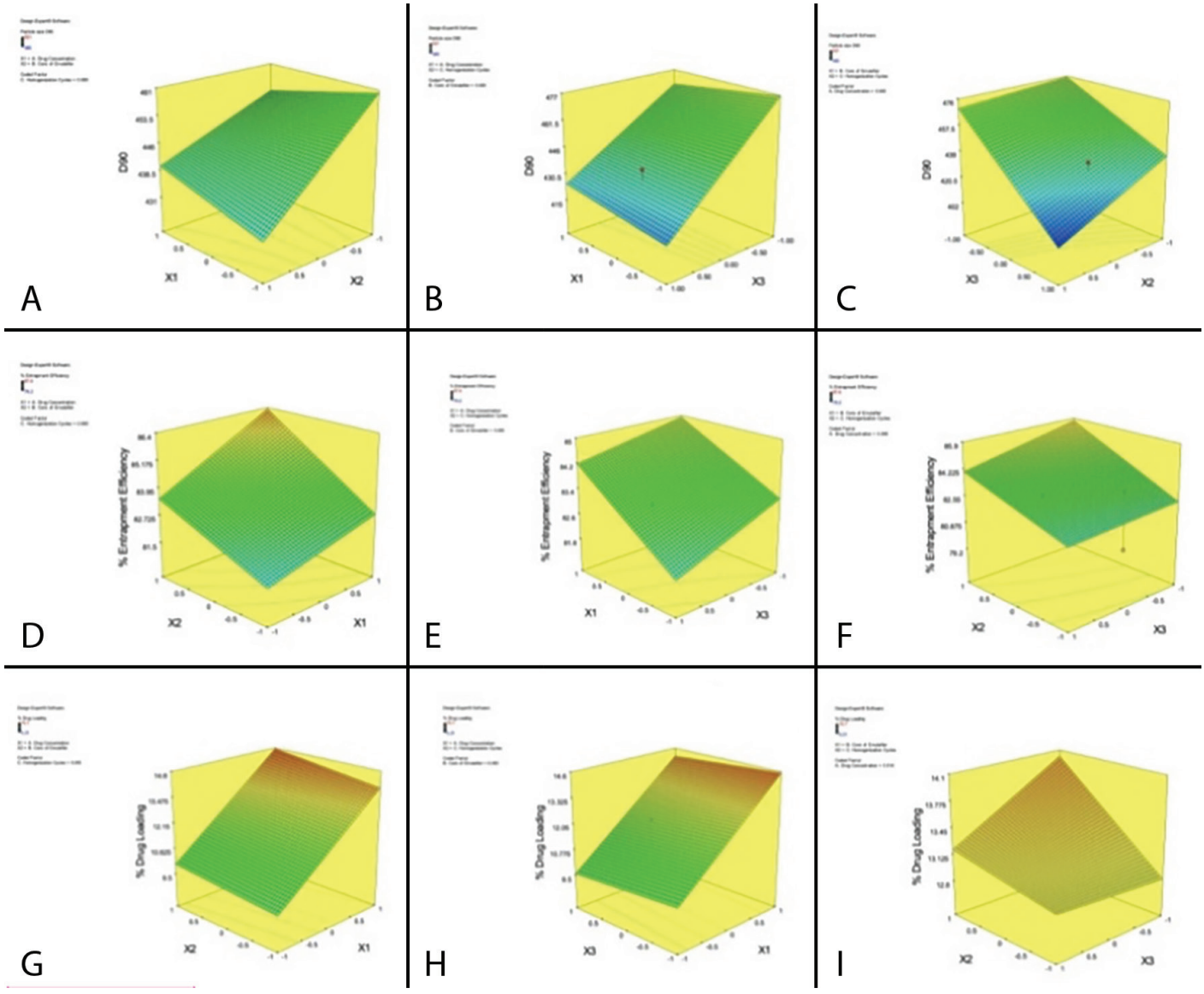

Figure 3. Effect of independent variables on particle size, EE%, and DL% (dependent variables)
EE: Entrapment efficiency, DL: Drug loading

result of greater homogenization cycles, which further cause drug leaching during the preparation of SLNs.

Optimization and validation

The 3D RSP results were based on polynomial models, which depicted the impact of significant independent factors on responses. Two additional checkpoint batches, P9 and P10, with the predicted values, were prepared to verify the validity of the optimization process. The checkpoint batches were prepared, and the variance between the observed and predicted values was examined using the Student's *t*-test (Table 2). The outcomes showed a high degree of closeness between observed and predicted values, and the difference between them was not significant ($p>0.05$). As a result, the obtained mathematical Equation was found to be accurate in predicting the responses Y_1, Y_2, and Y_3 (Table 3).

Table 3. Comparison of observed and predicted values of PYZ-SLNs (optimized batch P11) (mean ± SD, n=3)

Formulation	Characterisation		
	Y_1 (nm)	Y_2 (%)	Y_3 (%)
Batch P11 (Predicted value)	404	85.74	14.33
Batch P11 (Observed value)	401±08	86.24±1.15	14.38±0.85
Bias# %	0.75	-0.58	-0.35

#Bias % = (Predicted value - Observed value)/Observed value x 100, SD: Standard deviation, PYZ-SLNs: Pyrazinamide-loaded solid lipid nanoparticles

The software Design-Expert 10 (version 10.0.6) was used to create optimum conditions for PYZ-SLNs, with a desirability value of 0.878. The optimized batch P11 was selected by setting the criteria of particle size <500 nm, and DL% and

EE% as being the highest. For the optimization batch, the software projected the following process parameters: drug concentration (PYZ) =30% *w/w*, emulsifier concentration (Soy lecithin) =0.3% *w/v*, and homogenization cycles =12. Furthermore, the Design-Expert 10 software predicted that the optimized batch P11 would have a particle size of 404 nm (Figure 4), with 85.74% (EE%) and 14.33% (DL%). Table 3 shows that the predicted values produced by the software and the practical values (P11-optimized PYZ-SLNs) were in good agreement.

In vitro drug release analysis of PYZ-SLNs

The lyophilized PYZ-SLNs (batch P11) *in vitro* drug release study was conducted at different pH values: 1.2 (0.1 N HCl), 6.8, and 7.4 (PBS), 4.5 (citrate-phosphate buffer) (Figure 5A and B). At a pH of 1.2, the PYZ-SLNs (Batch P11) exhibited ~10% drug release in 2 h. However, at pH 4.5, 6.8, and 7.4, the PYZ-SLNs (Batch P11) were observed to have a biphasic drug release pattern, releasing about 90% of the drug in 5 days (120 h) at different pH ranges. This pattern consisted of an initial burst release (~30% in 12 h) and thereafter, a sustained release (~90% in 120 h). The drug release pattern was found to be the same in the entire pH range. Therefore, it was concluded that the *in vitro* release of PYZ-SLNs was pH-independent.

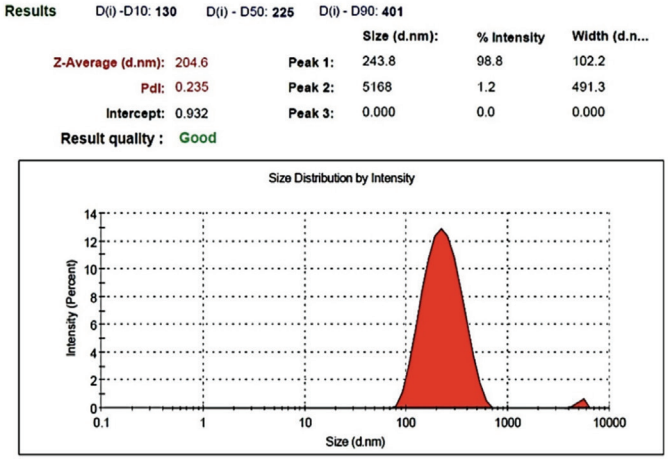

Figure 4. Particle size and particle size distribution of optimized PYZ-SLNs (Batch P11)

PYZ-SLNs: Pyrazinamide-loaded solid lipid nanoparticles

Drug release kinetics

Furthermore, the optimized PYZ-SLNs, (Batch P11), *in vitro* drug release profile was fitted to first-order, zero-order, Baker-Lonsdale, Hixson-Crowell, Korsmeyer-Peppas, Higuchi, and Weibull models (Table 4). To further describe the drug release mechanism, the best model with the lowest *f*-value and the highest R-square value was selected. The Hixson-Crowell model (Figure 5C) best fits the drug release profile of the PYZ-SLNs (Batch P11), with the lowest *f*-value and the highest R-squared when compared to other models (Table 4). The Hixson-Crowell model explains drug release through a dissolution mechanism, which depends on the surface area of the drug particles in contact with the aqueous phase. Hence, the larger the surface area, the faster the particle dissolution.[56,57]

DSC analysis

DSC analysis demonstrates the alterations in thermal behavior occurring because of the interactions amongst lipid components and drug during fabrication of PYZ-SLNs.[58-60] The pure PYZ transition temperature (Figure 6A) was determined to be 191.78 °C (endothermic peak) by DSC analysis.[61,62] The stearic acid (lipid excipient) transition temperature (Figure 6B) was determined to be 60.44 °C. Due to the addition of excipients such as soy lecithin and stearylamine (emulsifier), the blank SLNs peak (Figure 6C) was altered to 69.38 °C. Furthermore, in optimized PYZ-SLNs batch P11 (Figure 6D), the peak for the pure drug was not obtained. This might be attributed to the encapsulation of PYZ in a distributed form inside the SLN lipid core.

Morphological examination by TEM analysis

The TEM analysis of the PYZ-SLNs (batch P11) showed that the particles had a smooth surface and even size and shape (Figure 7A). There was no discernible particle aggregation, and the mean diameter was <500 nm. These analyses validate the outcomes of the DLS method.

PXRD analysis

The OriginPro 2017 software (OriginLab Corporation, USA) was used to analyze the diffraction patterns of the PYZ-SLNs (Batch

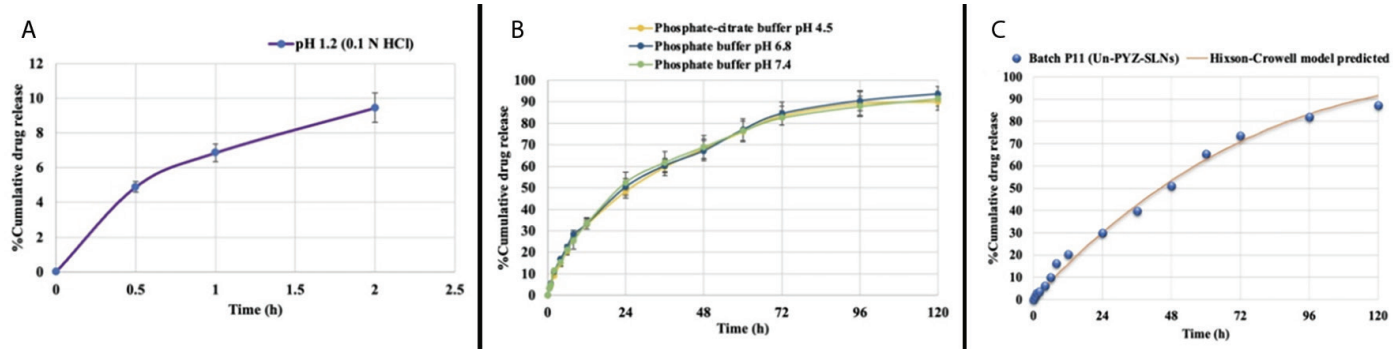

Figure 5. Dissolution profile of batch P11 in (A) pH 1.2 (0.1 N HCl), (B) phosphate-citrate buffer (pH 4.5) and phosphate buffer (pH 6.8 and 7.4); (C) Hixson-Crowell model for batch P11 (mean ± SD, n=3)

SD: Standard deviation

Table 4. *F*-values and R^2 of optimized PYZ-SLNs (batch P11) for different kinetic models

Parameters	Zero order model	First order model	Higuchi model	Hixcon-Crowell model	Korsmeyer-Peppas model	Baker lonsdale model	Weibull model
R^2	0.8923	0.9892	0.9695	0.9923	0.9861	0.9627	0.9683
F-value	544.83	23.80	114.22	11.65	24.18	102.48	120.74

PYZ-SLNs: Pyrazinamide-loaded solid lipid nanoparticles

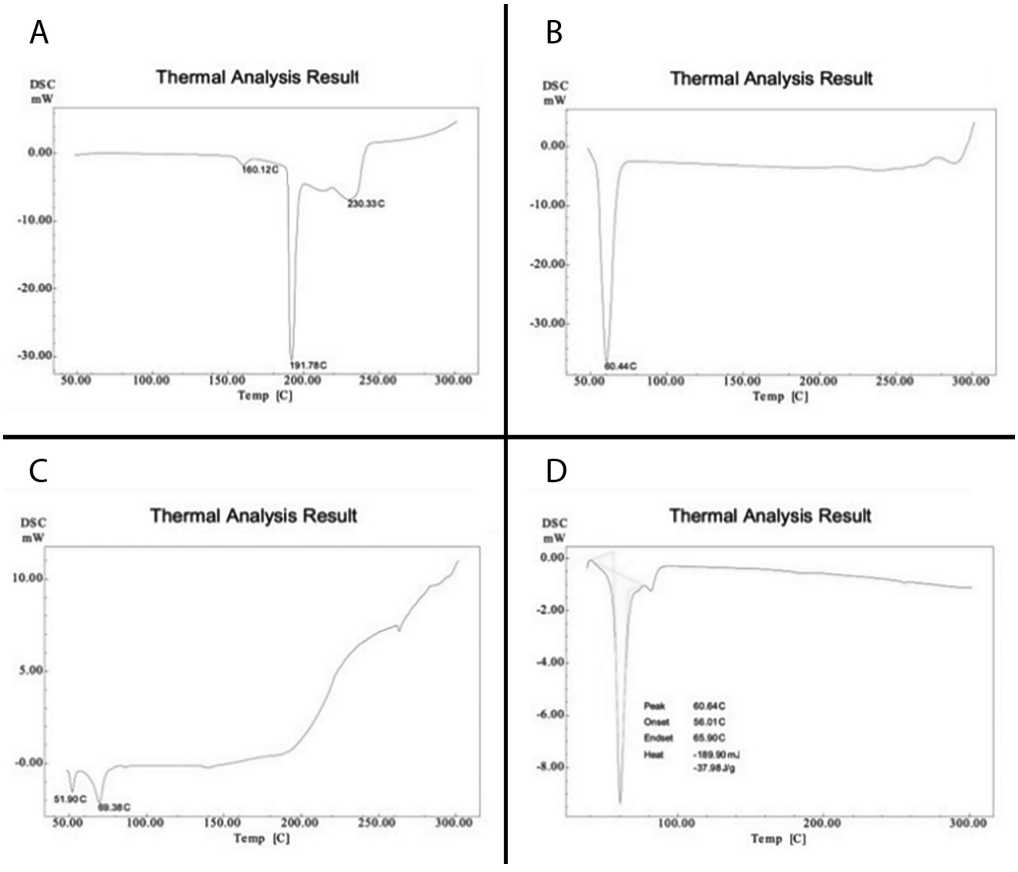

Figure 6. DSC of (A) pure PYZ powder, (B) stearic acid (lipid), (C) blank SLNs, (D) optimized PYZ-SLNs (batch P11)
DSC: Differential scanning calorimetry, PYZ-SLNs: Pyrazinamide-loaded solid lipid nanoparticles

P11) and PYZ, as shown in Figure 7B. The p-XRD patterns of PYZ showed its crystalline character, as clear sharp peaks were observed in the 2θ scale. In the PYZ-SLNs (Batch P11), the data showed a decline in the relative integrated peak intensity, and there was no discrete PYZ peak, signifying that PYZ was encapsulated in the lipid core of the SLNs in an amorphous form. Therefore, it can be concluded that the PYZ, which was incorporated into the lipid core of SLNs, was completely solubilized and changed into an amorphous state.

GI stability studies (in vitro)

PYZ-SLNs were uniformly distributed without any drug precipitation, according to the outcomes of stability studies (Table 5). Furthermore, after being incubated with different United States Pharmacopeia buffers, with a pH range of 1.2 to 7.4, statistically non-significant (p>0.05) variations in PDI values, EE%, and particle size were observed.

Stability studies for PYZ-SLNs

The stability of SLNs was determined at freezer (8 ˚C), intermediate conditions (30±2 ˚C/RH 65±5%), and accelerated conditions (40±2 ˚C/RH 75±5%) for 6 months. At predetermined intervals (initial, 1 month, 3 months, and 6 months), samples were analyzed for any alterations in physical appearance, ease of redispersibility, EE%, PDI, and particle size (D90). Table 6 represents the stability results for the lyophilized formulations (PYZ-SLNs). The lyophilized powder had a fluffy appearance, and upon reconstitution with water, it was found to be easily re-dispersed. Furthermore, there were no noteworthy changes in the parameters, suggesting that the prepared nanoparticles were stable and had a long shelf-life.

DISCUSSION

The PYZ-SLNs were fabricated using a high-pressure homogenization technique. In the preliminary trials, it was

Table 5. *In vitro* GI stability studies for PYZ-SLNs (batch P11) (mean ± SD, n=3)

Medium	Particle size (nm)		PDI		EE%	
	Pre-incubation	Post incubation	Pre-incubation	Post incubation	Pre-incubation	Post incubation
pH 1.2 (0.1 N HCl)	401±08	406±07	0.235±0.03	0.237±0.04	86.24±1.15	85.37±1.79
Sodium acetate buffer pH 4.5	401±08	404±06	0.235±0.03	0.238±0.03	86.24±1.15	85.70±0.64
Phosphate buffer pH 6.8	401±08	403±03	0.235±0.03	0.240±0.05	86.24±1.15	85.12±1.40
Phosphate buffer pH 7.4	401±08	404±09	0.235±0.03	0.236±0.04	86.24±1.15	85.29±1.62

GI: Gastrointestinal, SD: Standard deviation, PYZ-SLNs: Pyrazinamide-loaded solid lipid nanoparticles, EE: Entrapment efficiency, PDI: Polydispersity index

Table 6. Stability evaluation of PYZ-SLNs (batch P11) (mean ± SD, n=3)

Stability testing condition	PYZ-SLNs		
	Particle size (nm)	PDI	EE (%)
Initial*	401±08	0.235±0.03	86.24±1.15
5±3 °C**			
1 month	402±08	0.236±0.04	86.02±0.47
3 months	404±09	0.239±0.03	85.35±0.84
6 months	410±12	0.242±0.05	84.85±1.06
30±2 °C/65±5% RH**			
1 month	403±09	0.237±0.04	85.88±0.76
3 months	404±08	0.240±0.05	85.16±0.94
6 months	413±11	0.242±0.07	83.67±1.12
40±2 °C/75±5% RH**			
1 month	405±08	0.239±0.05	85.68±1.18
3 months	412±10	0.242±0.06	84.15±1.61
6 months	417±11	0.244±0.08	82.79±2.08

*: Fresh samples, **: Lyophilized samples, SD: Standard deviation, PYZ-SLNs: Pyrazinamide-loaded solid lipid nanoparticles, EE: Entrapment efficiency, PDI: Polydispersity index

observed that three parameters, namely, homogenization cycles, drug concentration, and emulsifier concentration, had a noteworthy impact on DL%, EE%, and particle size of PYZ-SLNs. A 2^3 factorial design was applied to optimize PYZ-SLNs. By employing Design-Expert software, the 3D response surface plots were generated and investigated. The independent variables emulsifier concentration (X_2) and homogenization cycles (X_3) had a significant reverse impact on particle size of PYZ-SLNs. With the increase in homogenization cycles, the decrease in particle size might be owing to the cavitation forces in the high-pressure homogenizer, leading to the reduction of PYZ-SLNs to nano-scale.[53,54] Moreover, an increase in emulsifier concentration reduced the particle size of PYZ-SLNs. This might be owing to increased stabilization of pre-emulsion by an emulsifier, leading to a diminution in particle size as well as its aggregation.[53] Furthermore, the drug concentration and emulsifier concentration had a positive impact on the EE% of PYZ-SLNs. The high drug solubilization and incorporation into the lipid core could be responsible for an increase in EE%.[53,55] The EE% decreased with an increase in homogenization cycles (X_3). This might be owing to the increased surface area of particles owing to the cavitational forces generated with increased cycles of homogenization resulting in drug leaching during SLN formation.[53,54] Thereafter, the impact of independent variables on DL% showed that an increase in drug concentration and emulsifier concentration led to an increase in DL%. The increase in drug concentration was attributed to more drug accessible to get incorporated into the lipid matrix. Furthermore, the drug gets solubilized more in the lipid matrix with the addition of an emulsifier as it acts as a solubilizer. Thus, an increase in emulsifier concentration increases the DL%. However, an increase in homogenization cycles led to a decrease in DL%. This could be the result of greater homogenization cycles which further cause drug leaching during the preparation of SLNs.[53,54]

To validate the optimization process, checkpoint batches (P9 and P10) with predicted values were prepared. The predicted and observed values represented a high degree of closeness

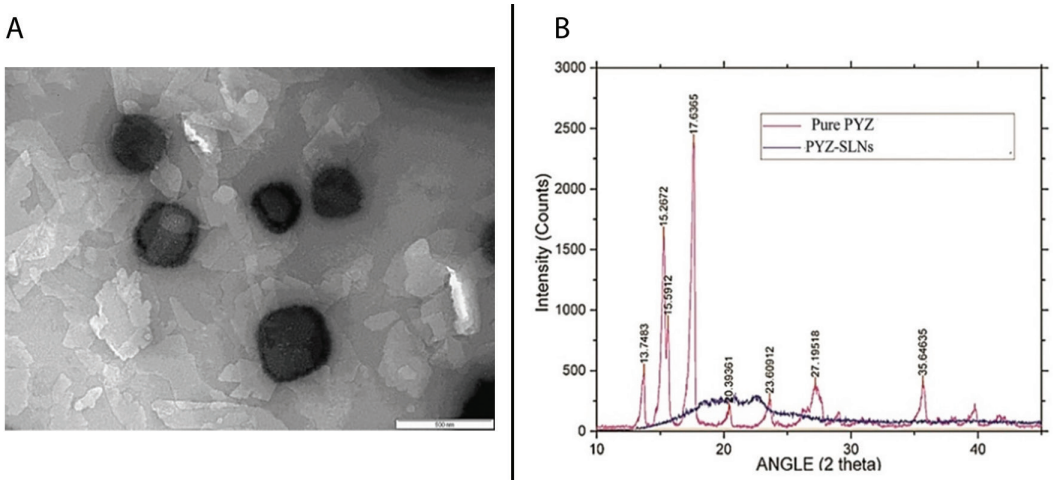

Figure 7. (A) TEM images of batch P11; (B) PXRD patterns of Pure PYZ and batch P11 (PYZ-SLNs)
TEM: Transmission electron microscopy, PXRD: Powder X-ray diffraction, PYZ-SLNs: Pyrazinamide-loaded solid lipid nanoparticles

as the difference among them was not significant (p>0.05). Thus, the obtained mathematical Equation was accurate in predicting the responses Y_1, Y_2, and Y_3. The optimized batch (P11) was fabricated by setting the optimum conditions (particle size: <500 nm and DL% and EE% of highest). The predicted and observed values of the P11 batch were in close agreement.

The *in vitro* drug release from the optimized batch P11 (lyophilized), evaluated in different pH media, represented an initial burst release followed by a sustained release. Further, the Hixson-Crowell model was found to provide the best fit for the PYZ-SLNs drug release profile as it had the highest R-square and lowest *f*-value. The Hixson-Crowell model explains the drug release by a dissolution mechanism, which depends on the outer surface of the aqueous phase. Hence, the larger the surface area, the faster the particle dissolution.[56,57] DSC analysis demonstrates the alterations in thermal behavior occurring because of the interactions among lipid components and drug during fabrication of PYZ-SLNs.[58-60] Herein, the DSC results of optimized PYZ-SLNs (P11 batch) did not show the peak of the pure drug. This might be attributed to the encapsulation of PYZ in a distributed form inside the SLNs lipid core.[61,62] Moreover, the TEM analysis results did not depict any particle aggregation. The TEM results validated the outcomes of the DLS method. The PXRD indicated a decrease in peak intensity and did not detect any PYZ peaks. Thus it was concluded that the PYZ was incorporated into the lipidic core of SLNs solubilized, and changed into an amorphous state. Furthermore, the PYZ-SLNs were determined to be stable under accelerated stability conditions for 6 months, as there were no changes in EE%, D90, PDI, or their physical appearance.

CONCLUSION

The current research work emphasizes the prospects of SLNs as an efficient carrier for oral delivery of the anti-tubercular drug PYZ. For optimizing the formulated PYZ-SLNs systematically, three factors and a two-level fractional factorial design were applied. The *in vitro* drug release study represented a biphasic release of PYZ-SLNs, consisting of an initial burst release followed by sustained release, fitting best with the Hixson-Crowell model, indicative of a release *via* a diffusion mechanism. The *in vitro* lipolysis analysis showed that PYZ-SLNs demonstrated an anti-lipolytic action in the fasted-state simulated intestinal (lipase-containing) fluid. PYZ-SLNs demonstrated good resistance *in vitro* and easily withstood varied GI tract-resembling media. The accelerated stability assessment confirmed that the PYZ-SLNs were stable even after 6 months, indicating their long shelf-life. Hence, from the aforementioned outcomes, it may be inferred that the optimized and formulated PYZ-SLNs can avert the PYZ degradation in varied GI media, and can be employed as a promising nano-based treatment for TB.

Ethics

Ethics Committee Approval: Not required.

Informed Consent: Not required.

Acknowledgment

Authors are thankful to the Institute of Pharmacy, Nirma University, Ahmedabad, Gujarat, India for providing the necessary facilities to generate the manuscript that is a part of Doctor of Philosophy (Ph.D.) research work of Mr. Nimitt Chokshi, submitted to Nirma University, Ahmedabad, India.

Footnotes

Authorship Contributions

Concept: N.C., M.P., Design: N.C., M.P., Data Collection or Processing: N.C., P.V., S.C., M.P., Analysis or Interpretation: N.C., P.V., M.P., Literature Search: N.C., S.C., Writing: N.C., P.V., S.C., M.P.

Conflict of Interest: The authors declare no conflicts of interest.

Financial Disclosure: The authors are highly grateful to Department of Science and Technology, Fund for Improvement of S&T Infrastructure (grant number: SR/FST/LSI-607/2014), Government of India for providing the necessary funding to establish equipment facility in laboratory.

REFERENCES

1. Programme GT. Global tuberculosis report 2023 [Internet]. 2023. Available from: https://iris.who.int/
2. El-Ridy MS, Abdelbary A, Nasr EA, Khalil RM, Mostafa DM, El-Batal AI, Abd El-Alim SH. Niosomal encapsulation of the antitubercular drug, pyrazinamide. Drug Dev Ind Pharm. 2011;37:1110-1118.
3. Rojanarat W, Nakpheng T, Thawithong E, Yanyium N, Srichana T. Inhaled pyrazinamide proliposome for targeting alveolar macrophages. Drug Deliv. 2012;19:334-345.
4. Sosnik A, Carcaboso AM, Glisoni RJ, Moretton MA, Chiappetta DA. New old challenges in tuberculosis: potentially effective nanotechnologies in drug delivery. Adv Drug Deliv Rev. 2010;62:547-559.
5. Thomas J, Bagyalakshmi J. Design, development and characterization of pyrazinamide niosomal dosage form. Am J Pharmtech Res. 2013;3:532-544.
6. Varma JN, Kumar TS, Prasanthi B, Ratna JV. Formulation and characterization of pyrazinamide polymeric nanoparticles for pulmonary tuberculosis: efficiency for alveolar macrophage targeting. Indian J Pharm Sci. 2015;77:258-266.
7. Chiang SS, Starke JR. Mycobacterium tuberculosis. In: Principles and Practice of Pediatric Infectious Diseases. Elsevier; 2023. p. 806-823.e4.
8. Zhang N, Savic RM, Boeree MJ, Peloquin CA, Weiner M, Heinrich N, Bliven-Sizemore E, Phillips PPJ, Hoelscher M, Whitworth W, Morlock G, Posey J, Stout JE, Mac Kenzie W, Aarnoutse R, Dooley KE; Tuberculosis Trials Consortium (TBTC) and Pan African Consortium for the evaluation of antituberculosis antibiotics (PanACEA) networks. Optimising pyrazinamide for the treatment of tuberculosis. Eur Respir J. 2021;58:2002013.
9. El-Ridy MS, Mostafa DM, Shehab A, Nasr EA, Abd El-Alim S. Biological evaluation of pyrazinamide liposomes for treatment of *Mycobacterium tuberculosis*. Int J Pharm. 2007;330:82-88.
10. Stehr M, Elamin AA, Singh M. Pyrazinamide: the importance of uncovering the mechanisms of action in mycobacteria. Expert Rev Anti Infect Ther. 2015;13:593-603.
11. Singh A, Das SS, Ruokolainen J, Kesari KK, Singh SK. Biopolymer-capped pyrazinamide-loaded colloidosomes: *In vitro* characterization and bioavailability studies. ACS Omega. 2023;8:25515-25524.
12. Pham DD, Fattal E, Tsapis N. Pyrazinamide-loaded poly(lactide-co-glycolide) nanoparticles: optimization by experimental design. J Drug Deliv Sci Technol. 2015;30:384-390.
13. Zielińska A, Carreiró F, Oliveira AM, Neves A, Pires B, Venkatesh DN, Durazzo A, Lucarini M, Eder P, Silva AM, Santini A, Souto EB. Polymeric nanoparticles: production, characterization, toxicology and ecotoxicology. Molecules. 2020;25:3731.
14. Traini D, Young PM. Drug delivery for tuberculosis: is inhaled therapy the key to success? Ther Deliv. 2017;8:819-821.
15. Date AA, Hanes J, Ensign LM. Nanoparticles for oral delivery: design, evaluation and state-of-the-art. J Control Release. 2016;240:504-526.
16. Reinholz J, Landfester K, Mailänder V. The challenges of oral drug delivery via nanocarriers. Drug Deliv. 2018;25:1694-1705.
17. Talegaonkar S, Bhattacharyya A. Potential of lipid nanoparticles (SLNs and NLCs) in enhancing oral bioavailability of drugs with poor intestinal permeability. AAPS PharmSciTech. 2019;20:121.
18. Shete H, Patravale V. Long chain lipid-based tamoxifen NLC. Part I: preformulation studies, formulation development and physicochemical characterization. Int J Pharm. 2013;454:573-583.
19. Khatak S, Mehta M, Awasthi R, Paudel KR, Singh SK, Gulati M, Hansbro NG, Hansbro PM, Dua K, Dureja H. Solid lipid nanoparticles containing anti-tubercular drugs attenuate the *Mycobacterium marinum* infection. Tuberculosis (Edinb). 2020;125:102008.
20. Pandey R, Khuller GK. Solid lipid particle-based inhalable sustained drug delivery system against experimental tuberculosis. Tuberculosis (Edinb). 2005;85:227-234.
21. O'Neil MJ. An Encyclopedia of Chemicals, Drugs, and Biologicals. The Merck Index, 14th edition. 2006.
22. Zhang Z, Lu Y, Qi J, Wu W. An update on oral drug delivery *via* intestinal lymphatic transport. Acta Pharm Sin B. 2021;11:2449-2468.
23. Patel K, Padhye S, Nagarsenker M. Duloxetine HCl lipid nanoparticles: preparation, characterization, and dosage form design. AAPS PharmSciTech. 2012;13:125-133.
24. Rawal S, Patel B, Patel MM. Fabrication, optimisation and *in vitro* evaluation of docetaxel and curcumin co-loaded nanostructured lipid carriers for improved antitumor activity against non-small cell lung carcinoma. J Microencapsul. 2020;37:543-556.
25. Mathur P, Sharma S, Rawal S, Patel B, Patel MM. Fabrication, optimization, and *in vitro* evaluation of docetaxel-loaded nanostructured lipid carriers for improved anticancer activity. J Liposome Res. 2020;30:182-196.
26. Sinhmar GK, Shah NN, Chokshi NV, Khatri HN, Patel MM. Process, optimization, and characterization of budesonide-loaded nanostructured lipid carriers for the treatment of inflammatory bowel disease. Drug Dev Ind Pharm. 2018;44:1078-1089.
27. Kovacevic A, Savic S, Vuleta G, Müller RH, Keck CM. Polyhydroxy surfactants for the formulation of lipid nanoparticles (SLN and NLC): effects on size, physical stability and particle matrix structure. Int J Pharm. 2011;406:163-172.
28. Silva A. Segregated delivery of rifampicin and isoniazid from fixed dose combination bilayer tablets for the treatment of tuberculosis. Br J Pharm Res. 2014;4:1781-1801.
29. Vinchhi P, Patel JK, Patel MM. High-pressure homogenization techniques for nanoparticles. In: Emerging Technologies for Nanoparticle Manufacturing. Cham: Springer International Publishing; 2021. p. 263-285.
30. Gaspar DP, Faria V, Gonçalves LM, Taboada P, Remuñán-López C, Almeida AJ. Rifabutin-loaded solid lipid nanoparticles for inhaled antitubercular therapy: physicochemical and *in vitro* studies. Int J Pharm. 2016;497:199-209.
31. Singh H, Jindal S, Singh M, Sharma G, Kaur IP. Nano-formulation of rifampicin with enhanced bioavailability: development, characterization and *in-vivo* safety. Int J Pharm. 2015;485:138-151.
32. Sinhmar GK, Shah NN, Rawal SU, Chokshi NV, Khatri HN, Patel BM, Patel MM. Surface engineered lipid nanoparticle-mediated site-specific drug delivery system for the treatment of inflammatory bowel disease. Artif Cells Nanomed Biotechnol. 2018;46:565-578.
33. Khatri H, Chokshi N, Rawal S, Patel MM. Fabrication, characterization and optimization of artemether loaded PEGylated solid lipid nanoparticles for the treatment of lung cancer. Mater Res Express. 2019;6:045014.
34. Chokshi NV, Khatri HN, Patel MM. Formulation, optimization, and characterization of rifampicin-loaded solid lipid nanoparticles for the treatment of tuberculosis. Drug Dev Ind Pharm. 2018;44:1975-1989.

35. Pinheiro M, Ribeiro R, Vieira A, Andrade F, Reis S. Design of a nanostructured lipid carrier intended to improve the treatment of tuberculosis. Drug Des Devel Ther. 2016;10:2467-2475.

36. Prabhakar K, Afzal SM, Kumar PU, Rajanna A, Kishan V. Brain delivery of transferrin coupled indinavir submicron lipid emulsions-pharmacokinetics and tissue distribution. Colloids Surf B Biointerfaces. 2011;86:305-313.

37. Subedi RK, Kang KW, Choi HK. Preparation and characterization of solid lipid nanoparticles loaded with doxorubicin. Eur J Pharm Sci. 2009;37:508-513.

38. Ravi PR, Aditya N, Kathuria H, Malekar S, Vats R. Lipid nanoparticles for oral delivery of raloxifene: optimization, stability, *in vivo* evaluation and uptake mechanism. Eur J Pharm Biopharm. 2014;87:114-124.

39. Luo Y, Chen D, Ren L, Zhao X, Qin J. Solid lipid nanoparticles for enhancing vinpocetine's oral bioavailability. J Control Release. 2006;114:53-59.

40. Garanti T, Stasik A, Burrow AJ, Alhnan MA, Wan KW. Anti-glioma activity and the mechanism of cellular uptake of asiatic acid-loaded solid lipid nanoparticles. Int J Pharm. 2016;500:305-315.

41. Gao Y, Sarfraz MK, Clas SD, Roa W, Löbenberg R. Hyaluronic acid-tocopherol succinate-based self-assembling micelles for targeted delivery of rifampicin to alveolar macrophages. J Biomed Nanotechnol. 2015;11:1312-1329.

42. Jain A, Agarwal A, Majumder S, Lariya N, Khaya A, Agrawal H, Majumdar S, Agrawal GP. Mannosylated solid lipid nanoparticles as vectors for site-specific delivery of an anti-cancer drug. J Control Release. 2010;148:359-367.

43. Kumar PV, Asthana A, Dutta T, Jain NK. Intracellular macrophage uptake of rifampicin loaded mannosylated dendrimers. J Drug Target. 2006;14:546-556.

44. Vandal OH, Nathan CF, Ehrt S. Acid resistance in *Mycobacterium tuberculosis*. J Bacteriol. 2009;191:4714-4721.

45. Zhang Y, Huo M, Zhou J, Zou A, Li W, Yao C, Xie S. DDSolver: an add-in program for modeling and comparison of drug dissolution profiles. AAPS J. 2010;12:263-271.

46. Zhang X, Chen G, Zhang T, Ma Z, Wu B. Effects of PEGylated lipid nanoparticles on the oral absorption of one BCS II drug: a mechanistic investigation. Int J Nanomedicine. 2014;9:5503-5514.

47. Benito-Gallo P, Franceschetto A, Wong JC, Marlow M, Zann V, Scholes P, Gershkovich P. Chain length affects pancreatic lipase activity and the extent and pH-time profile of triglyceride lipolysis. Eur J Pharm Biopharm. 2015;93:353-362.

48. Kalaria DR, Sharma G, Beniwal V, Ravi Kumar MN. Design of biodegradable nanoparticles for oral delivery of doxorubicin: *in vivo* pharmacokinetics and toxicity studies in rats. Pharm Res. 2009;26:492-501.

49. Abdelwahed W, Degobert G, Fessi H. Investigation of nanocapsules stabilization by amorphous excipients during freeze-drying and storage. Eur J Pharm Biopharm. 2006;63:87-94.

50. Müller RH, Maassen S, Weyhers H, Mehnert W. Phagocytic uptake and cytotoxicity of solid lipid nanoparticles (SLN) sterically stabilized with poloxamine 908 and poloxamer 407. J Drug Target. 1996;4:161-170.

51. Torcello-Gómez A, Maldonado-Valderrama J, Jódar-Reyes AB, Foster TJ. Interactions between Pluronics (F127 and F68) and bile salts (NaTDC) in the aqueous phase and the interface of oil-in-water emulsions. Langmuir. 2013;29:2520-2529.

52. Wu B, Liu H, Chen G, Zhang Y, Ma Z. Effects of PEGylated lipid nanoparticles on the oral absorption of one BCS II drug: a mechanistic investigation. Int J Nanomedicine. 2014;5503.

53. Chavan SS, Ingle SG, Vavia PR. Preparation and characterization of solid lipid nanoparticle-based nasal spray of budesonide. Drug Deliv Transl Res. 2013;3:402-408.

54. Vivek K, Reddy H, Murthy RS. Investigations of the effect of the lipid matrix on drug entrapment, *in vitro* release, and physical stability of olanzapine-loaded solid lipid nanoparticles. AAPS PharmSciTech. 2007;8:E83.

55. Rowe RC, Sheskey PJ, Quinn ME. Handbook of pharmaceutical excipients. The Pharmaceutical Press and the American Pharmaceutical Association. 2009;6th ed.

56. Barzegar-Jalali M, Adibkia K, Valizadeh H, Shadbad MR, Nokhodchi A, Omidi Y, Mohammadi G, Nezhadi SH, Hasan M. Kinetic analysis of drug release from nanoparticles. J Pharm Pharm Sci. 2008;11:167-177.

57. Ferreira M, Chaves LL, Lima SA, Reis S. Optimization of nanostructured lipid carriers loaded with methotrexate: A tool for inflammatory and cancer therapy. Int J Pharm. 2015;492:65-72.

58. Jose S, Prema MT, Chacko AJ, Thomas AC, Souto EB. Colon specific chitosan microspheres for chronotherapy of chronic stable angina. Colloids Surf B Biointerfaces. 2011;83:277-283.

59. Patel MM. Formulation and development of di-dependent microparticulate system for colon-specific drug delivery. Drug Deliv Transl Res. 2017;7:312-324.

60. Xu J, Bovet LL, Zhao K. Taste masking microspheres for orally disintegrating tablets. Int J Pharm. 2008;359:63-69.

61. Alves R, Reis TV da S, Silva LCC da, Storpírtis S, Mercuri LP, Matos J do R. Thermal behavior and decomposition kinetics of rifampicin polymorphs under isothermal and non-isothermal conditions. Braz J Pharm Sci. 2010;46:343-351.

62. Silva AM, Vieira B, Carmo FA, Amaral L, Silva LCRP, Escudini CS, Lopes M, Rodrigues CR, Ribeiro AJ, Cabral L. Segregated delivery of rifampicin and isoniazid from fixed dose combination bilayer tablets for the treatment of tuberculosis. Br J Pharm Res. 2014;4:1781-1801.